Egyptian Geophysical Society
EGS Journal, Vol. 18, No. 1, 1-11 (2020)

ESTIMATION AND INTERPRETATION OF RADIOACTIVE HEAT PRODUCTION USING AIRBORNE GAMMA-RAY SURVEY DATA OF G. UMM ANAB - G. EL DOB REGION, CENTRAL EASTERN DESERT, EGYPT

N.H. EL GENDY[(1)], M.A.S. YOUSSEF[(2)], Sh.T. ELKHODARY [(1)] and Th.A.M. SHAMS EL DEEN[(1)]

(1) Geology Department, Faculty of Science, Tanta University, Tanta 31527, Egypt

(2) Nuclear Materials Authority, Exploration Division, P.O. Box 530, Maadi, Cairo, Egypt.

تقييم وتفسير الانتاج الحراري المشع باستخدام بيانات المسح الاشعاعي الجوي لأشعه جاما لمنطقه جبل أم عنب – جبل الدوب، وسط الصحراء الشرقية، مصر

الخلاصـــــة: يتناول هذا العمل رسم خرائط وتقييم الإنتاج الحراري المشع من الصخور في منطقة جبل أم عنب – جبل الدب – وسط الصحراء الشرقية – مصر، باستخدام بيانات مسح أشعة جاما الطيفية الجوية. وبعد فصل بيانات المسح الاشعاعي الجامي الطيفية للكل وحدة صخرية والحصول على قيمة الكثافة النوعية لها. أظهرت النتائج أن الاشعاع الحرارى في المنطقة يتراوح من ٠,١٤ مايكرو وات لكل متر مكعب إلى ٥,٥٠ مايكرو وات لكل متر مكعب ويتواجد اعلى اشعاع حرارى فى هذة الصخور الجرانيتية و الصخور الميتا جابرو للميتادايوريت حيث يتراوح المتوسط العام للإنتاج الحراري المشع من هذه الصخور من ١,٢٠ مايكرو وات لكل متر مكعب الى ١,٥٠ مايكرو وات لكل متر مكعب. بينما بلغت القيم المتوسطة للاشعاع الحرارى الناتج من صخور حمامات الرسوبية، الدخان البركاني والميتاجابرو المتداخلة والميتافولوكانك حيث تتراوح قيم الاشعاع الحراي الناتج من الصخور من٠,٨٠ لكل متر مكعب الي ١,٢٠ مايكرو وات لكل متر مكعب و قد سجلت أقل قيم للمتوسط العام للاشعاع الحرارى الناتج من الوحدات الصخرية (اقل من ٠,٨٠ مايكرو وات لكل متر مكعب) في رسوبيات الوديان والصخور الرسوبية (مكون ام مهرا ومكون التاريف) والميتاسيدمنت، صخور الجابرو والصخور المتحولة. وتبين من أستخدام الطريقتين أن نتائج الطريقتين متقاربة لدرجة كبيرة. كما لاحظ ايضا وجود مصاحبة للصخور ذات الانتاج الحراري مع أماكن زيادة الثلاثة تركيزات للعناصر المشعة معا (مكافئ اليورانيوم ومكافئ الثوريوم والبوتاسيوم) والعكس صحيح.

ABSTRACT: *The present work deals with mapping the radioactive heat production from rocks in Gabal (G.) Umm Anab - G. El Dob area at the central Eastern Desert of Egypt, using the airborne spectrometric gamma-ray survey data. The results show that, the radioactive heat production in the areas ranges from 0.14 μWm^{-3} to 5.50 μWm^{-3}. In the granites, metagabbro to metadiorite in the western part of Gabal Umm Anab has abnormally high radioactive heat production values varying from 2.10 μWm^{-3} to 4.19 μWm^{-3}. Meanwhile, the higher averages of radioactive heat production of these rock units change from 1.20 μWm^{-3} to 1.50 μWm^{-3}. The intermediate averages of heat production of Hammamat sediments, metavolcanics, intrusive metagabbro, and Dokhane volcanics have values ranging from 0.80 μWm^{-3} to 1.20 μWm^{-3}. The lowest average values of heat production less than 0.80 μWm^{-3} and are found in the Quaternary deposits, metavolcanics, sedimentary rocks, meta sediments, gabbroic rocks (fresh olivine gabbro and troctolite). Umm Mahara Formation, melanocritic medium-to high-grade metamorphic rocks and Taref Formation.*

1. INTRODUCTION

The investigated area is situated at the central Eastern Desert of Egypt (Fig. 1) and lies between latitudes 26° 36\\\- 27° 00\\\N and longitudes 33°- 34° E. More than 95% of the area is covered by igneous and metamorphic rocks. The remaining 5% is covered by sedimentary rocks, as wadi sediments.

The study area was mapped by the Egyptian Geological Survey and Mining Authority (EGSMA, 1992). The objectives of this study are to identify the contact areas among various rock types in the G.Umm Anab - G. El Dob area and to map the radioactive heat production, using the spectral radiometric measurements extracted from the airborne spectral gamma-ray survey data of the area (Aero-Service, 1984).

2. GEOLOGIC SETTING

The study area is a part of the central Eastern Desert of Egypt (Fig. 1). Geologically, the area is described as both low hills, as well as high and rugged mountains. This area is covered by an assortment of igneous, metamorphic and sedimentary rocks, that range in age from Precambrian to Quaternary. The Egyptian Geological Survey and Mining Authority (EGSMA, 1992) distributed the geographical guide, demonstrating the distribution of different rock units in the examined area (Fig. 2).

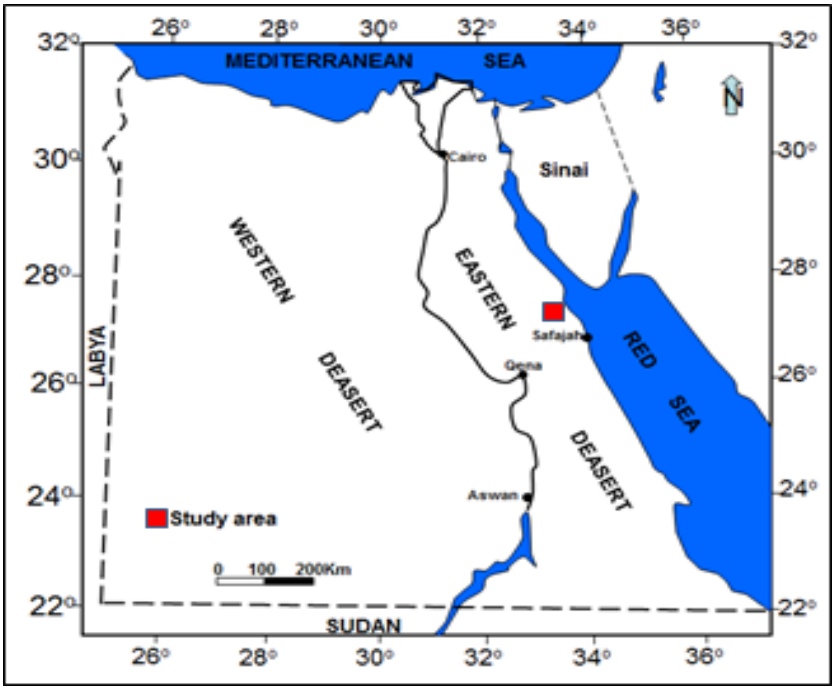

Fig. 1: Location map of the study area.

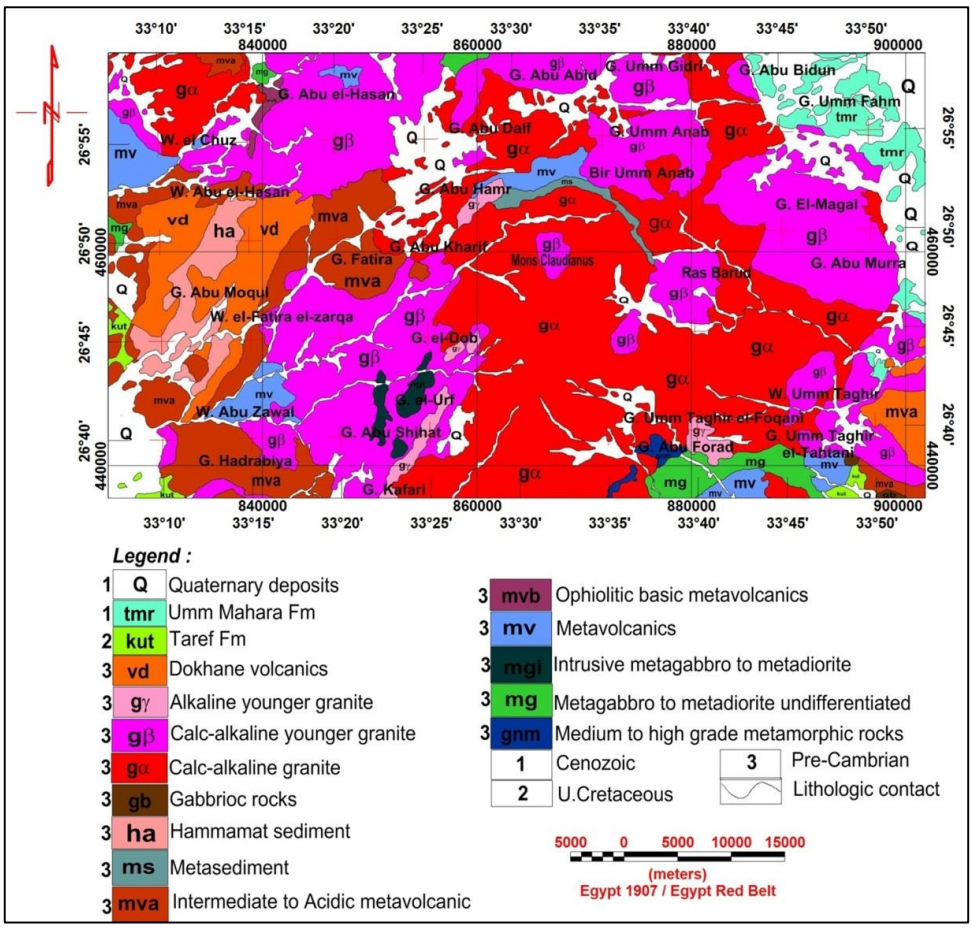

Fig. 2: Geologic Map of G. Umm Anab-El Dob area, Central Eastern Desert, Egypt. (EGSMA, 1992).

Stratigraphically, the Late Proterozoic (Precambrian) rocks comprise most of the study area, covering 80% of the investigated area, with melanocritic medium to high grade metamorphic rocks (gnm), metagabbro to metadiorite, undifferentiated (mg), intrusive metagabbro to metadiorite (mgi), metavolcanics, undifferentiated intermediate to acid metavolcanics and metapyroclastics (mv), Ophiolitic basic metavolcanics (mvb), Intermediate to acid metavolcanics and metapyroclastics (mva), metasediment metamorphosed shelf sediments and volcanogenic rocks, partly including pyroclastics (ms), Hammamate clastics, molasse-type conglomerate to siltstone sequence (Ha), Gabbroic rocks, fresh olivine gabbro, norite and troctolite (gb), calc-alkaline, usually quartz dioritic to granodioritic rocks, also previously "Grey granite" or "Older granite" in part, deeply weathered (gα), calc-alkaline and weakly deformed granitic rocks. Also, previously pink granite or younger granite in part, deeply weathered (gβ), alkaline, generally undeformed granitic to alkali-feldspare granitic rocks, previously pink granite or younger granite in part, deeply weathered (gγ), Dokhane volcanics. Calc-alkaline andesitic to rhyolitic rocks (vd), (EGSMA, 1992). The Upper Cretaceous sedimentary rocks cover the southern part of the study area with Taref Formation (kut) comprising mainly sandstone. Also, the southwestern and southeastern parts are covered by Taref Fm., while the southwestern, central and northeastern parts of the study area are underlain by Tertiary Rocks such as well as Umm Mahara Formation. Reefal and algal carbonate rock with bioclastics. Underlain by Ranga Formation siliciclastic fanglomerates and interfan siltstone and sandstone (Tmr) and Undiff. Quaternary deposits (Q), along vallies (Fig. 2)

Structurally, the investigated area was affected by different tectonics, giving rise to complex structures. For instance, the area is cut by various types of faults, which define wadis and drainage lines or cut through the country rocks (Fig. 3.1). The faults are mainly of thrust and normal types and trend in the NE-SW direction, as a major trend and a minor trend in the NNW-SSE directions (Fig.3.2) (EGSMA, 1992).

3. AIRBORNE GEOPHYSICAL SURVEY

The airborne gamma-ray spectrometric survey was conducted along parallel flight lines oriented in the NE-SW direction at 1.5 km intervals; The tie lines were flown in the NW-SE direction, at 10 km intervals. Spectral radiometric measurements were made at 300 feet (92.6 m) sampling interval and at a nominal sensor at a latitude of 120 m. These data were set up for consequent handling by digitizing the maps in numerical configuration, which allows the utilization of addition (gridding) technique.

The data were rectified for the background radiation coming about, because of the cosmic rays and aircraft defilement, varieties caused by the changes in the aircraft altitude, relative to the ground and the compton scattering gamma-rays in potassium and uranium vitality windows. The uranium and thorium concentrations are, therefore, expressed as equivalent concentrations, eU and eTh, in part of the radioactive material per million parts of rock (ppm). Potassium (K) is processed to produce the equivalent ground concentrations in percent (%). The corrected data give a gauge of the clear surface convergence of potassium, equivalent uranium and equivalent thorium (K, eU and eTh).

4. ESTIMATION AND INTERPRETATION OF RADIOGENIC HEAT PRODUCTION

The radiometric data were subjected to different techniques of processing and analysis, which include:

1. Creation of the radioelements (K, eU and eTh) shading maps.
2. Foundation of the radioelements, composite image maps (K, eU and eTh).
3. Detachment of eU, eTh and K aeroradiometric estimations over each lithologic unit.
4. Determination of their statistical characteristics, such as arithmetic mean (X) and standard deviation (S), and checking the normality of distribution of the measurements of rock units, using the coefficient of variability test.
5. Estimation, mapping and interpretation of the surface radioactive heat production from the airborne gamma-ray data for different rocks in the area.

5. AIRBORNE RADIOSPECTROMETRIC MAPS

Fig. (4) Demonstrates the false-shading radio spectrometric map for TC, that defines three class levels of high, intermediate and low. The abnormal state of more than 8.8 ppm is related to Calc-Alkaline younger granite (gβ), Alkaline younger granite (gγ), small parts of Calc-Alkaline granite (gα), parts of Taref Formation, Ophiolitic basic metavolcanics (mvb) and Umm Mahara Formation (Tmr). The intermediate level which ranges from 8.8 to 5.3 ppm is associated mainly with Quaternary deposits (Q), Hammamat group (ha) sediments, calc-alkaline granite (gα), dokhane volcanics (vd), The generally low level of less than 5.3 ppm is for the over intrusive metagabbro to metadiorite (mgi), metagabbro to metadiorite undifferentiated (mg), metasediment (ms), gabbroic rocks, fresh olivine gabbro, norite and troctolite (gb).

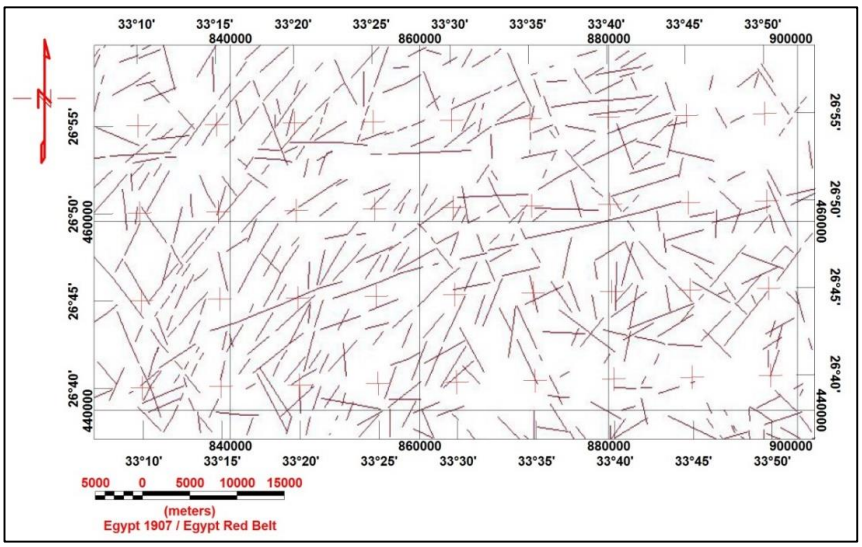

Fig. 3.1: Structural Features of G. Umm Anab-El Dob area, Central Eastern Desert, Egypt. (EGSMA, 1992).

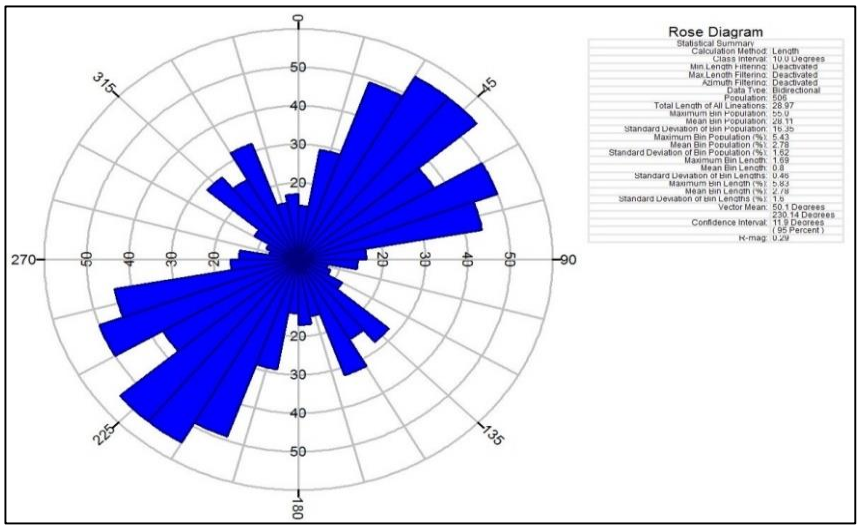

Fig. 3.2: Rose Diagram of G. Umm Anab-El Dob area, Central Eastern Desert, Egypt.

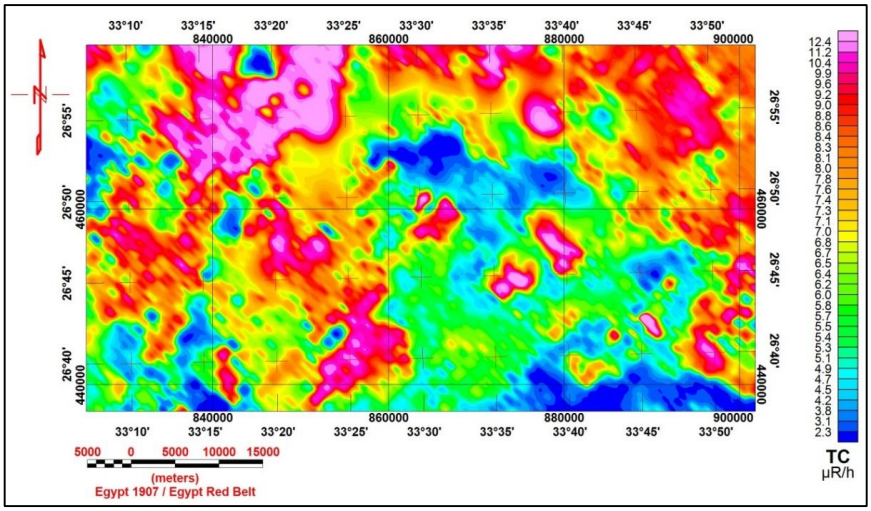

Fig. 4: Filled false colour radiometric map of TC, in µR/h, of G. Umm Anab-El Dob area, Central Eastern Desert, Egypt, (Aero-Service, 1984).

Melanocritic medium-to high-grade metamorphic rocks (gnm), intermediate to acid metavolcanics and metapyroclastics (mv), intermediate to basic metavolcanics (mva) and Taref Formation (kut).

The false-colour K radiospectrometric map (Fig. 5) shows the overall spatial distribution of the relative potassium concentrations in the study area. It indicates that, Taref Fm (kut), metasediment metamorphosed shelf sediments (ms), melanocritic medium-to high-grade metamorphic rocks (gnm), intermediate to basic metavolcanics (mva), intermediate to acid metavolcanics and metapyroclastics (mv), intrusive metagabbro to metadiorite (mgi) metagabbro to metadiorite undifferentiated (mg), gabbroic rocks, fresh olivine gabbro norite and troctolite (gb) and parts of Quaternary deposits (Q) represent generally low level (less than 1.61 %). The intermediate levels ranging from 1.61 to 2.65% are associated with Quaternary deposits, sediments of the Hammamat Group (ha), calc-alkaline granite (gα), parts of calc-alkaline younger granite (gβ), ophiolitic basic metavolcanics(mvb), parts of Dokhane volcanics (vd), and additionally the other parts Taref Formation (kut). The high K concentrations (more than 2.65%) are associated with calc-alkaline younger granite (gβ), alkaline younger granite (gγ), large parts of Dokhane volcanics, large parts of Quaternary deposits (Q), reefal and algal carbonate rock with bioclastic Underlain by Ranga Formation, siliciclastic fanglomerates and interfan siltstone and sandstone (Tmr), in which the false shading radiometric map of K concentrations coincides with the boundaries of these rock types.

The false-shading radiospectrometric map for eU defines three class levels of high, intermediate and low. The abnormal state, of in excess of 3.11 ppm, is related to calc-alkaline younger granite (gβ), alkaline younger granite(gγ), parts of Taref Formation(kut), some parts Quaternary deposits(Q), small parts of intermediate to basic metavolcanics (mva), ophiolitic basic metavolcanics (mvb), small parts of intermediate to basic metavolcanics (mva).The intermediate level, ranging from 1.48 to 3.11 ppm, is associated mainly with Quaternary deposits and Hammamat Group (ha) sediments, parts of calc-alkaline granite (gα), Taref Formation (kut), Dokhane volcanics (vd), parts of alkaline younger granite(gγ) and intermediate to basic metavolcanics(mva) The moderately low levels with estimations of less than 1.48 ppm, are over intrusive metagabbro to metadiorite (mgi), metagabbro to metadiorite undifferentiated (mg), metasediment (ms), gabbroic rocks, fresh olivine gabbro, norite and troctolite (gb). melanocritic medium-to high-grade metamorphic rocks (gnm), intermediate to acid metavolcanics and metapyroclastics (mv)and parts of calc-alkaline granite (gα).

Similar distribution is seen in the eTh through the false color radio spectrometric map (Fig. 7) The high level up to 8.6 ppm is associated with the Calc-Alkaline younger granite (gβ), Alkaline younger granite (gγ), parts of Calc-Alkaline granite (gα), parts of Taref Formation (kut), Ophiolitic basic meta volcanics (mvb). While the intermediate levels that range from 4.7 to 8.6 ppm is restricted to Quaternary deposits(Q), Hammamat group (ha) sediments, , melanocritic medium-to high-grade metamorphic rocks (gnm), intermediate to acid metavolcanics and metapyroclastics (mv), Calc-Alkaline granite (gα), Taref Formation (kut), Dokhane volcanics(vd), Intermediate to basic metavolcanics (mva). The low levels of less than 4.7 ppm linked with intrusive metagabbro to metadiorite (mgi), metagabbro to metadiorite undifferentiated (mg), metasediment (ms), gabbroic rocks, fresh olivine gabbro, norite and troctolite (gb).

Fig. 8 shows a false shading ternary radioelements image map, that joins the three radioelements (K, eU and eTh). Generally, the ternary plots of the radio-elements usually give a superior image of the geology; Separate radioelements maps are additionally valuable in distinguishing diverse rock units. For instance, the limits between different rock units can be outlined from the eU map (Fig. 4) while, the K and eTh maps (Figs. 3 and 5) illustrate the boundaries between the igneous and metamorphic rocks clearly. In the Gabal Umm Anab-Gabal El Dob area, higher uranium values extend to more than 3.2 ppm over areas underlain by granites.

5.1. Estimating radioactive heat production by the first method:

The first method of Rybach (1976) published an empirical relationship to calculate the radioactive heat production of a given rock sample, using this expression:

$$A\ (\mu W m^{-3}) = \rho\ (0.0952 c_u + 0.0256 c_{Th} + 0.0348 c_K) \quad (1)$$

Where: ρ is the dry density of rock (g/cm3) and C is the concentrations of eU and eTh in ppm and K in %, respectively. In the Rybach's relation, it is necessary first to know the density and the concentrations of the three radioelements: U, Th and K in the rock. Radioactive heat production was calculated from the concentrations of radioelements measured in the laboratory (Fernandez et al., 1998) and directly from the gamma-ray logs (Bücker and Rybach, 1996). Besides, the radioactive heat production was later assessed from airborne gamma-ray data, using the recipe of (Rybach, 1976); Richardson and Killeen, 1980; Thompson et al., (1996) and Salem et al., (2005). To ascertain the radioactive heat production from airborne gamma-ray survey data, both the types of rocks and their limits must be identified well beforehand. Moreover; the average density for each rock unit should be known, and computed in lab Shaaban.

Figure 9 and Table 1 show the radioactive heat production, related to each rock unit (μWm-3) in the investigated area. Near review of the figured midpoints of the apparent heat production values, evaluated in, this examination; demonstrates that, for the crustal rocks, contrasted with values calculated by Rybach (1976) shows the following relationships.

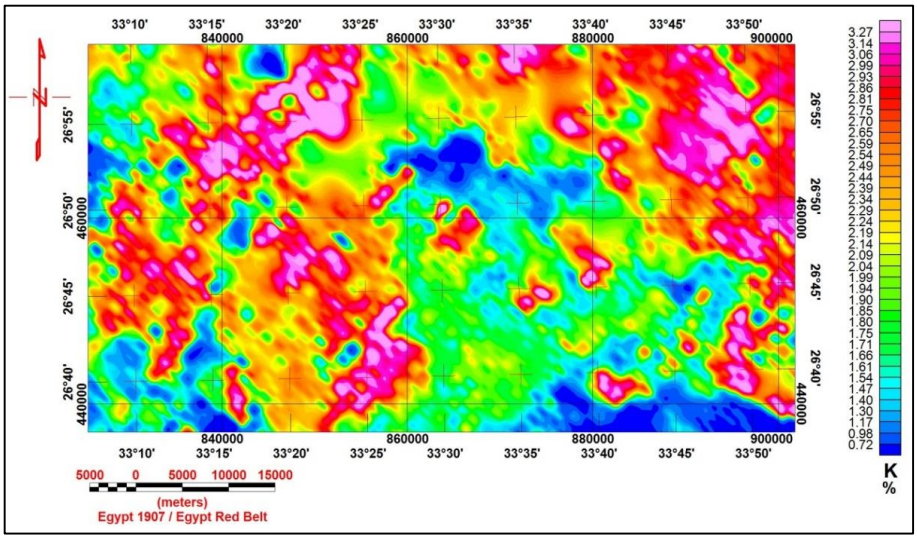

Fig. 5: Filled false colour radiometric map of K, in (%), of G. Umm Anab-El Dob area, Central Eastern Desert, Egypt, (Aero-Service, 1984).

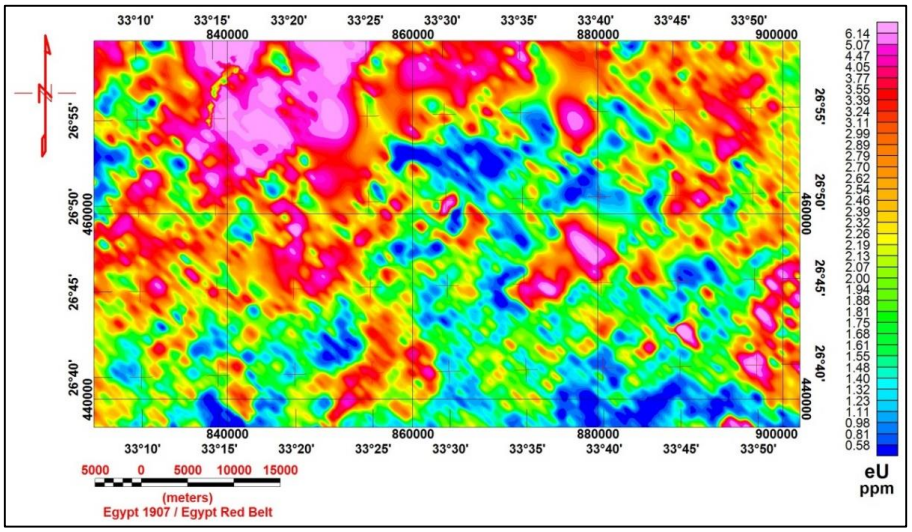

Fig. 6: Filled false colour radiometric map of eU, in (ppm) of G. Umm Anab-El Dob area, Central Eastern Desert, Egypt, (Aero-Service, 1984).

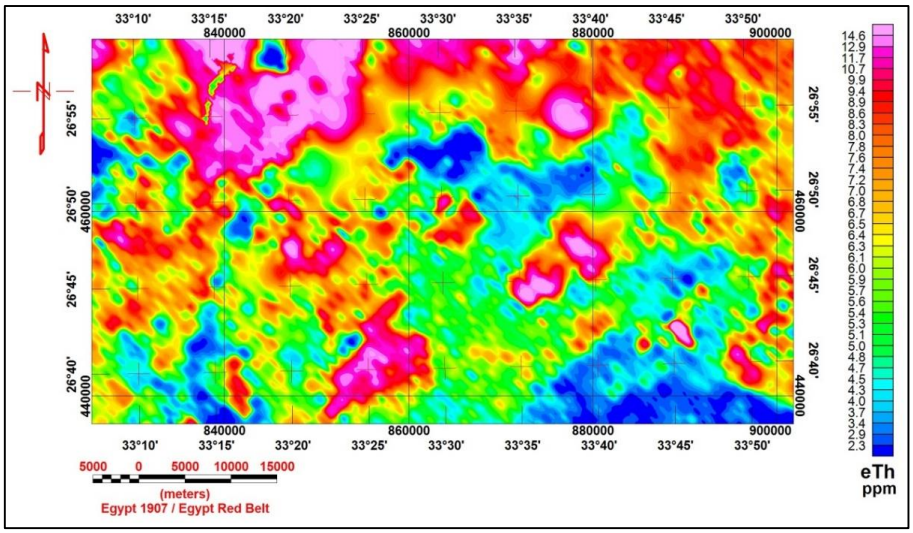

Fig. 7: Filled false colour radiometric map of eTh, in (ppm), of G. Umm Anab-El Dob area, Central Eastern Desert, Egypt, (Aero-Service, 1984).

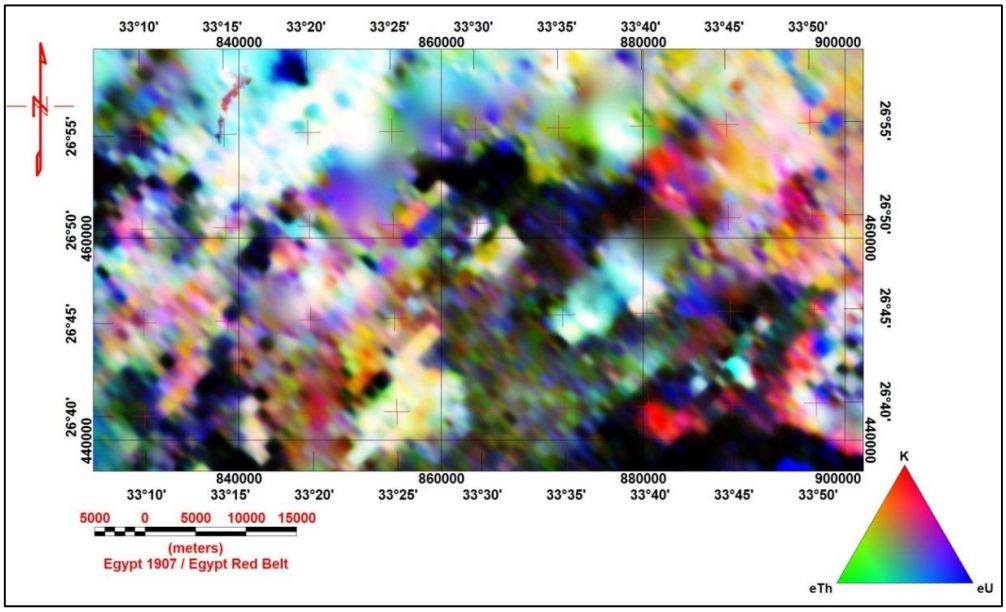

Fig. 8: Filled false colour Ternary radioelement image map of G. Umm Anab-G. El Dob area, Central Eastern Desert, Egypt.

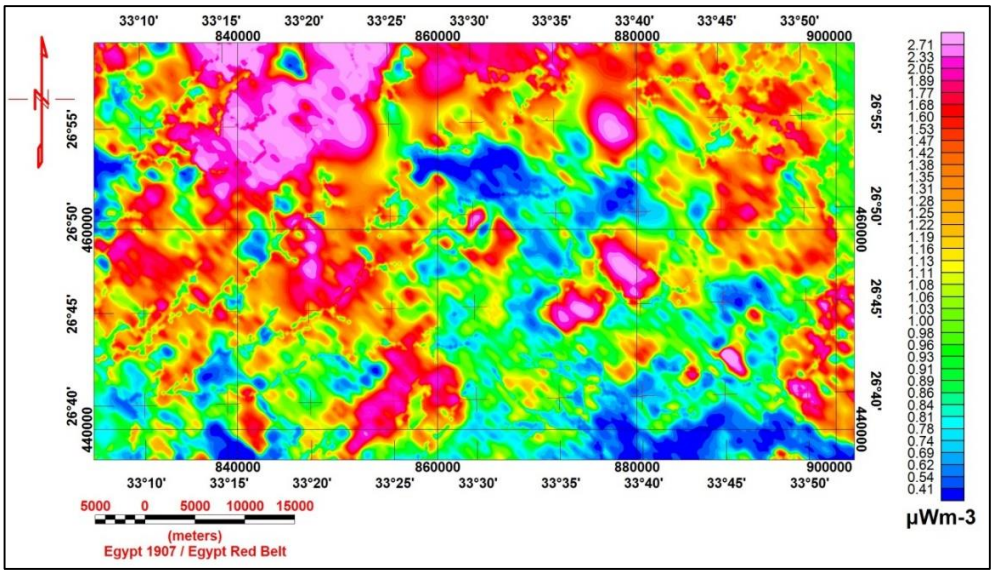

Fig. 9: Calculated RHP colour map calculated from Rybach (1976) of G.Umm Anab-G. El Dob area, Central Eastern Desert, Egypt.

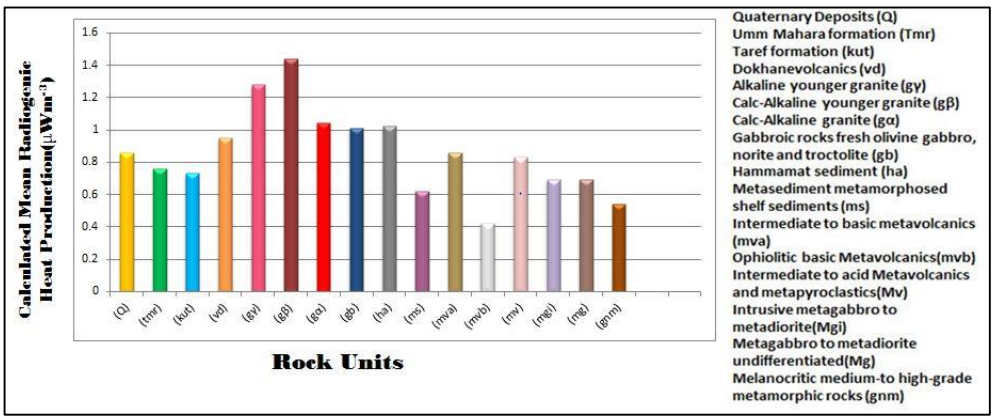

Fig. 10: Histogram show the average means of the RHP of by calculated from Rybach (1976), G. Umm Anab-G. El Dob Area, Central Eastern Desert, Egypt.

Table 1: Radioactive heat production corresponding to each rock units (in μWm^{-3}) calculated by Rybach (1976).

No.	Rock Units	Groups	Density gm./cm^3	No. of Samples	Calculated Radioactive Heat Production (μWm^{-3})				CV. (%)	Estimated general Level
					(X)	(S)	Range			
							Min.	Max.		
1	Quaternary deposits (Q)	Sediment	1.92	1072	0.86	0.24	0.44	2.18	27.77	Intermediate
2	Umm Mahara Formation (Tmr)	Sedimentary	1.35	1459	0.76	0.23	0.25	1.79	30.66	Low
3	Taref Formation (kut)			108	0.73	0.24	0.35	1.52	32.79	Low
4	Dokhane volcanics (vd)	Volcanics	2.60	237	0.95	0.18	0.48	1.72	19.09	Intermediate
5	Alkaline younger granite (gγ)	Granite	2.64	767	1.28	0.54	0.18	3.49	42.17	High
6	Calc-Alkaline younger granite (gβ)			27883	1.44	0.65	0.16	5.17	38.84	High
7	Calc-Alkaline granite (gα)			16427	1.04	0.37	0.20	5.50	36.18	Intermediate
8	Gabbroic rocks fresh olivine gabbro, norite and troctolite (gb)	Olivine gabbro	3.03	268	1.01	0.16	0.20	2.05	38.38	Intermediate
9	Hammamat sediment (ha)	Hammamat	2.61	147	1.02	0.27	0.50	1.44	17.15	Intermediate
10	Metasediment metamorphosed shelf sediments (ms)	Meta Sediment	2.62	247	0.62	0.29	0.15	1.38	47.18	Low
11	Intermediate to basic metavolcanics (mva)	Meta Volcanics	2.78	2642	0.86	0.32	0.14	2.28	37.79	Intermediate
12	Ophiolitic basic metavolcanics(mvb)			152	0.42	0.26	0.15	1.31	62.53	Low
13	Intermediate to acid Metavolcanics and metapyroclastics(Mv)		2.74	1722	0.83	0.44	0.15	2.81	53.47	Intermediate
14	Intrusive metagabbro to metadiorite(Mgi)	Metagabbro to Metadiorite	2.88	213	0.99	0.42	0.31	1.23	26.32	Intermediate
15	Metagabbro to metadiorite undifferentiated(Mg)			896	0.69	0.54	0.17	4.05	78.23	Low
16	Melanocritic medium-to high-grade metamorphic rocks (gnm)	Gneiss	2.80	138	0.54	0.18	0.26	1.06	34.05	Low

Min. = Minimum Value, Max. = Maximum Value, (X) = Mean, (S) = Standard Deviation, C.V. = Coefficient of Variability, Low Level (values less than 0.8 µWm-3), Intermediate Level (Values from 0.8 to 1.2 µWm-3) and high levels (Values more than 1.2 µWm-3).

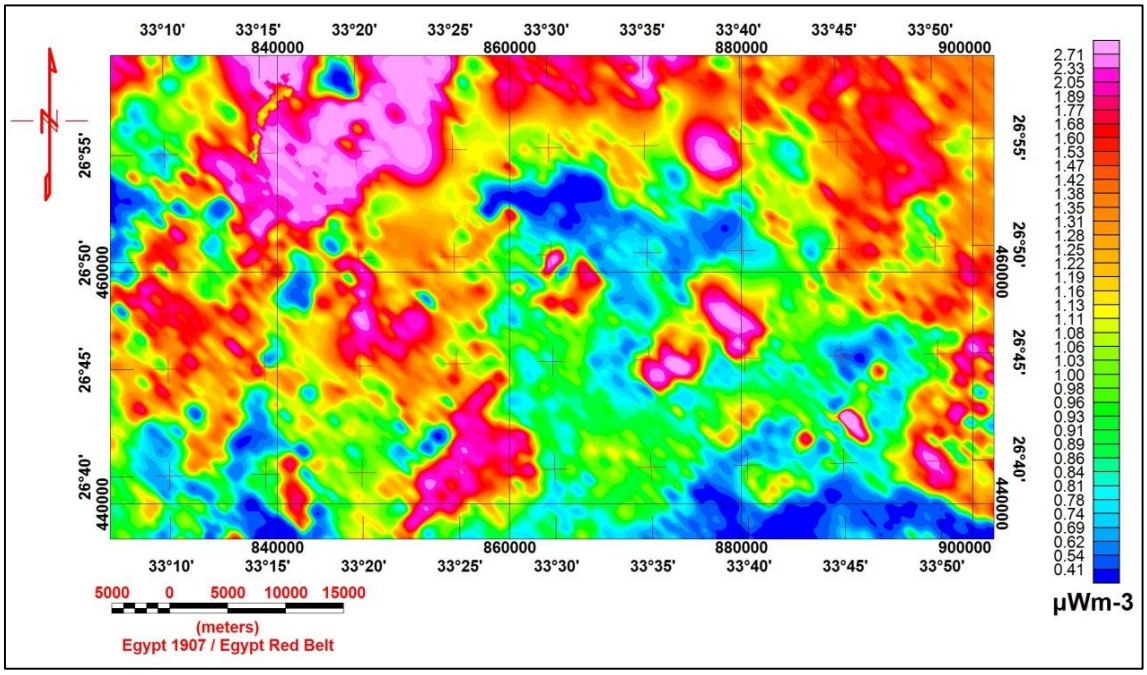

Fig. 11: Radioactive heat production colour map calculated from Bücker and Rybach (1996) of G. Umm Anab - G. El Dob area, Central Eastern Desert, Egypt.

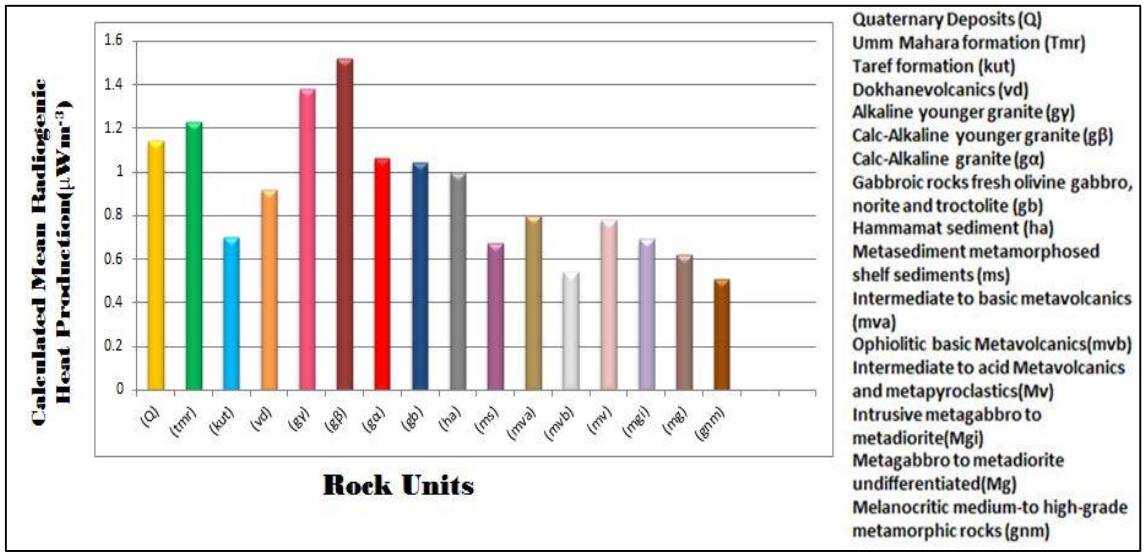

Fig. 12: Histogram show the average means of the radioactive heat production corresponding to each rock unit by calculated from Bücker and Rybach (1996).

5.2. Estimating radioactive heat production from Bücker and Rybach method:

The second method (Fig. 11) depends on total gamma-ray emission that reflects the combined radioactive decay of uranium, thorium and potassium, may be used in calculating Radiogenic Heat Production (RHP). An option of experimental relationship was distributed by Bücker and Rybach (1996) relates the bulk RHP rate to the total gamma-ray emission (TC) recorded by borehole tools as:

$$RHP\ [\mu W/m\text{-}3] = 0.0158\ (TC\ [API] - .8) \qquad (2)$$

Where API unit is the American petroleum institute, the standard equation of (API unit) calculated by Ellis, 1987 is

$$API = 16 * K\ (\%) + 8 * U\ (ppm) + 4 * Th\ (ppm) \qquad (3)$$

To ascertain the radioactive heat production from airborne gamma-ray data, each type of rocks and their limits must be known in advance. Additionally, the average density for each rock unit (Table.2) should be known or can be assumed. The study area consists of large separable units of igneous and metamorphic rocks, as well as ranges of sedimentary rocks.

Table (2): Radioactive heat production corresponding to each rock units (in µWm-3) calculated from Bücker and Rybach (1996).

No.	Rock Units	Groups	Density gm./cm^3	No. of Samples	Calculated Radioactive Heat Production (µWm^{-3})				CV. (%)	Estimated general Level
					(X)	(S)	Range			
							Min.	Max.		
1	Quaternary deposits (Q)	Sediment	1.92	1072	1.14	0.18	0.77	2.17	16.40	Intermediate
2	Umm Mahara Formation (Tmr)	Sedimentary	1.35	1459	0.96	0.19	0.42	1.88	19.82	Intermediate
3	Taref Formation (kut)			108	0.70	0.16	0.40	1.29	24.00	Intermediate
4	Dokhane volcanics (vd)	Volcanics	2.60	237	0.92	0.14	0.49	1.31	15.22	Intermediate
5	Alkaline younger granite (gγ)	Granite	2.64	767	1.38	0.47	0.23	2.86	33.96	High
6	Calc-Alkaline younger granite (gβ)			27883	1.52	0.42	0.19	3.98	27.74	High
7	Calc-Alkaline granite (gα)			16427	1.06	0.32	0.27	4.19	30.16	Intermediate
8	Gabbroic rocks fresh olivine gabbro, norite and troctolite (gb)	Olivine gabbro	3.03	268	1.04	0.40	0.21	2.05	38.85	Intermediate
9	Hammamat sediment (ha)	Hammamat	2.61	147	1.00	0.17	0.55	1.34	17.54	Intermediate
10	Metasediment metamorphosed shelf sediments (ms)	Meta Sediment	2.62	247	0.67	0.34	0.15	1.33	50.96	Low
11	Intermediate to basic metavolcanics (mva)	Meta Volcanics	2.78	2642	0.80	0.27	0.17	1.83	34.32	Intermediate
12	Ophiolitic basic metavolcanics (mvb)			152	0.54	0.22	0.28	1.19	41.87	Low
13	Intermediate to acid Metavolcanics and metapyroclastics (Mv)		2.74	1722	0.78	0.40	0.14	2.24	51.54	Low
14	Intrusive metagabbro to metadiorite (Mgi)	Metagabbro to Metadiorite	2.88	213	0.69	0.17	0.28	1.12	24.97	Low
15	Metagabbro to metadiorite undifferentiated (Mg)			896	0.62	0.41	0.18	3.00	66.85	Low
16	Melanocritic medium-to high-grade metamorphic rocks (gnm)	Gneiss	2.80	138	0.51	0.17	0.25	0.94	33.69	Low

Min. = Minimum Value, Max. = Maximum Value, (X) = Mean, (S) = Standard Deviation, C.V. = Coefficient of Variability, Low Level (values less than 0.8 µWm-3), Intermediate Level (Values from 0.8 to 1.2 µWm-3) and high levels (Values more than 1.2 µWm-3).

6. CONCLUSIONS

New insights on the geothermal distribution pattern of G. Umm Anab-G. El Dob area were based on the existing airborne spectral gamma-ray data for identifying the suitable rock units generating the radioactive heat maps. The radiogenic heat production (RHP) in the investigation area depends on the decay of the isotopes of potassium K, Uranium eU and Thorium eTh, the generated heat values range from 0.14 to 5.50 mWm^{-3} The highest RHP values are estimated in parts underlain by muscovite rich rocks (1.50 mWm^{-3}). The intermediate RHP is recorded in parts over Hammamat sediments, metavolcanics, intrusive metagabbro, Dokhane volcanic, with RHP values ranges from 0.8 μWm^{-3} to1.20 μWm^{-3}. The lowest average values of heat production values are less than 0.80 $\mu Wm^{-3}$and originating from the following rock units: Quaternary deposits, metavolcanics, sedimentary rocks, metasediment, gabbroic rocks (fresh olivine gabbro, norite and troctolite). Umm Mahara Formation, melanocritic medium-to high-grade metamorphic rocks and Taref Fm.

REFERENCES

Aero-Service, April, 1984: Final operational report of airborne magnetic/radiation survey in the Eastern Desert, Egypt for the Egyptian General Petroleum Corporation. Aero-Service, Houston, Texas. Six Volumes.

Bücker, C., Rybach, L., 1996: A simple method to determine heat production from gamma-ray logs. Mar. Pet. Geol. 13, 373-375.

Egyptian Geological Survey and Mining Authority (EGSMA), 1992: Geologic Map of Al Qusayr Quadrangle, Egypt.

Fernandez, M., Marzan, I., Correia, A., Ramalho, E., 1998: Heat flow, heat production and lithosphere thermal regime in the Iberian Peninsula. Tectonophysics 291, 29-53.

Richardson, K.A., Killeen, P.G., 1980: Regional radiogenic heat production mapping by airborne gamma-ray spectrometry. In: Current Research, Part B, Geological Survey of Canada, Paper 80-1B.227-232.

Rybach, L., 1976. Radioactive heat production in rocks and its relation to other Petrophysical parameters. Pure Appl. Geophys. 114, 309-318.

Salem, A., El Sirafy, A., Aref, A., Ismail, A., 2005: Mapping radioactive heat production from airborne spectral gamma-ray data of Gabal Duwi area, Egypt. In: Proceedings World Geothermal Congress, Antalya, Turkey, 24-29.

Shaaban, M.A., 1973: Geophysical studies on the Lead Zinc Mining District between Qusseir and Mersa Alam, Red Sea Coast, Eastern Desert, Egypt. Ph.D. Thesis No 568. Cairo University, Geizh, Egypt.

Thompson, P.H., Judge, A.S., Charbonneau, B.W., Carson, J.M., Thomas, M.D., 1996: Thermal regimes and diamond stability in the Archean slave province, Northwestern Canadian Shield, District of Mackenzie, Northwest Territories. In: Current Research, 96-1E, Geological Survey of Canada, 135-146.

Web site

http://www.engineeringtoolbox.com/mineral-density-d_1555.html.

http://www.engineeringtoolbox.com/density-solids-d_1265.html.

http://wiki.chemprime.chemeddl.org/index.php/Density_of_Rocks_and_Soils.